Reduced State Space Model of Interleaved Helical Transformer Winding

P. Bodlovic, K. Hot and T.Kelemen
Electrical Engineering Dept., Polytechnic of Zagreb, Croatia; e-mail: pbodlovi@tesla.vtszg.hr

***Abstract*: The reduced state space model of interleaved helical transformer winding enable to study the reflections of the traveling waves on the terminals and the crossover irregularities. The analytical eigenvalue-eigenvector analysis of the two-dimensional blocks of the transition matrix gives oscillating modes, their periods and damping.**

***Keywords*: interleaved winding, state-space, eigenvalues**

I. INTRODUCTION

Interleaving the turns of the transformer winding, proposed by the English Electric Co., is one of the constructive measures used to suppress atmospheric over-voltages due to free oscillations excited by the difference between the initial exponential and the final steady-state linear voltage distribution [1]. Interleaved winding construction, consisting of a coil wound from two parallel, crossed over, conductors increases the effective series capacitances between turns, making the initial voltage distributions closer to the linear. The effective increase of the serial capacitances is estimated [1] to be proportional to the second power of the number of turns in the winding. No method for computing the transients has been suggested.

The numeric computation of the voltage transients in the interleaved winding [2] is based on the multi-conductor transmission-line theory in the frequency domain.. The numerical results are confirmed with the experiments on a real interleaved winding. Both methods show oscillatory behavior of the transients The oscillations are imputed to some unexplained resonant conditions.

Simplified multi-conductor transmission-line model for the helical interleaved transformer winding in the time domain [3] approaches the origin of the oscillations. The crossing of the conductors is taken as a discrete irregularity that produces reflections of the traveling waves. The quasi-stationary multi-component states take place between reflections of the waves on the winding terminals and conductor crossing. The model describes the reduced state in terms of the surge voltage and the previous winding state through a low order system of the ordinary linear equations. The agreement with the full model is achieved for the first few steps only.

This work promotes the reduced state space model up to the eigenvalue analysis which brings to the light the primary properties of the associated dynamics, all in pure analytical form. Since effectively increased serial capacitances results in substantial raise of the charging surge currents it was assumed the resistances have essential influence on the dumping of the free oscillations.

The results are obtained in three phases.

The first phase creates the initial system of linear equations which consider the resistances to be lumped and supplemented to the terminal resistances. The total number of eight equations follows from the laws for the multiconductor traveling current and voltage waves of transversal electromagnetic field (TEM) according to the reduced model with the constant current waves inside the winding.

The next, most demanding phase, brings the initial system of linear equations to the standard discrete time state space form[4]:

$$[x(t+1) = [A][x(t) + [B][v \tag{1}$$

$$[y(t) = [C][x(t) + [D][v \tag{2}$$

where [x is the column vector of the state variables, [v is the column vector of the inputs (surge voltage) and [y is the column vector of the outputs. The efforts were aimed to find the state space of minimal dimension with state variables grouped into weakly coupled clusters. It has been found that only weak coupling exists between the two-dimensional even and two-dimensional odd parity state variables in the four-dimensional state space for the model with symmetrical resistances. With the weak coupling ignored the transition matrix [A] becomes block-diagonal.

In the final phase the analytical eigenvalue-eigenvector analysis of the two-dimensional blocks of the transition matrix [A] is performed giving oscillating modes, their periods and damping. The coupling between odd-even modes due to eventual skew-symmetric component of resistances can be analyzed according to the perturbation theory [5].

II. MULTI-CONDUCTOR TRANSMISSION LINE MODEL OF THE INTERLEAVED HELICAL WINDING

Interleaved helical winding having even number N of turns is constructed by winding N/2 turns of the two parallel conductors A and B and connecting the end of the last turn of the conductor A to the beginning of the first turn of the conductor B. By cutting the winding cylinder along the generator opposite to the terminals the winding can be developed in the plane as a multi-conductor transmission line shown in Fig. 1a). With a minor modification, shown in Fig 1.b), the crossover irregularity is separated from the terminal irregularity giving a more favorable, similar to the one in Ref. [4], multi-conductor transmission line representation of interleaved N+1 turns helical winding. The electromagnetic transients are represented by line currents $_{n}i(x,t)$ and voltages $_{n}e(x,t)$ to the grounded screen as functions of longitudinal coordinate x and time t. Subscript "n" is at the same time the discrete transversal coordinate n = 0,1....N . . Longitudinal coordinate "x" is continuous in the interval [0,w) where w is the length of each turn. The interleaving crossover is positioned at x = h = w/2. The coordinate x = h-0 is designated as g.

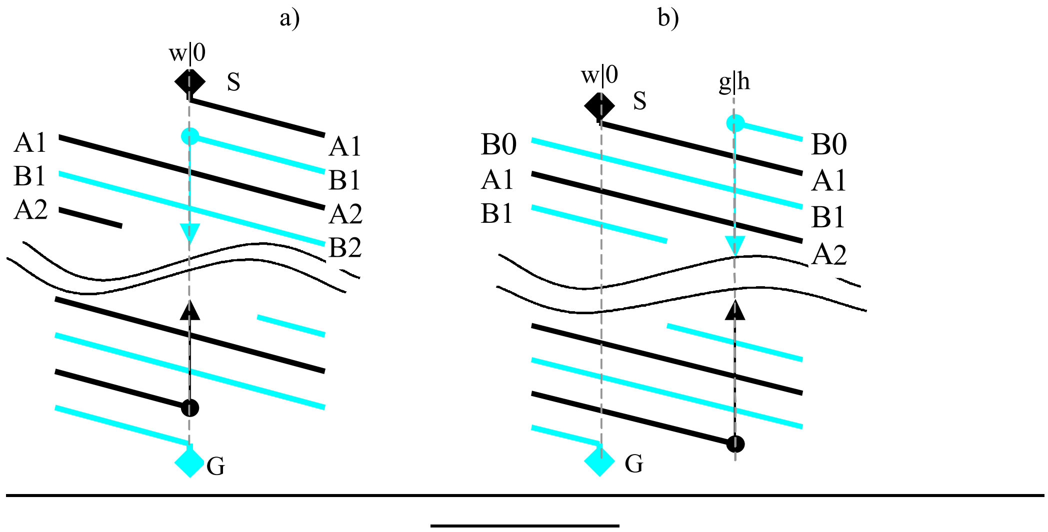

Figure. 1 Initial a) and modified b) multi-conductor transmission line model of the interleaved helical winding

Except discrete irregularities at x = 0,w and x = h, the transients ${}_{n}i\,(x,t)$ and ${}_{n}e\,(x,t)$ are supposed to satisfy the vector telegraphist's equations for homogenous lossless lines. The method of characteristics gives the solutions as the superposition of forward and backward traveling waves. In the TEM approximation these waves propagate undistorted between irregularities with the universal constant propagation velocity v and the surge impedance [Z] according to.

$$[i = [i_{\mathrm{f}} + [i_{\mathrm{b}};\ [e = [e_{\mathrm{f}} + [e_{\mathrm{b}}$$

$$[e_{\mathrm{f}} = [Z]\ [i_{\mathrm{f}}\,,\ \ [e_{\mathrm{b}} = -[Z]\ [i_{\mathrm{b}}$$

In the per unit system the surge impedance matrix [Z_{h}] is advantageously approximated [1,3] with

$${}_{n}Z_{hn} = \zeta^{|n-m|}$$

where ζ is the magnetic and the electric coupling constant being equal for the TEM waves.

Boundary conditions for the waves at the nodes influenced with the winding irregularities produce large scale system of linear equations. Since wave reflections occur only in the narrow boundary layers effectively only the small scale systems of equations have to be solved. In addition the penetrating currents reach quasi-stationary state that is quantitatively considered in the next section.

III. QUASI-STATIONARY INPUT –OUTPUT

The main result of this section is the matrix equation (7) for quasi-stationary outputs consisting of the four traveling electric currents waves penetrating into the depth of the winding in terms of the inputs consisting of the surge voltage ES, the ground voltage EG = 0 and the four electric currents waves coming from the depth of the winding. The development of the equation (7) is supported by the drawing in Figure 2 which introduces the variables in the surge terminal side of the winding in Figure 1b. The variables of the ground terminal side are introduced according the symmetry with the variables of the surge terminal side. The currents I_{AGf} and I_{BGf} are input waves in the A and B conductor to the ground terminal G while the currents i_{AGb} and i_{BGb} are the outputs. The crossover current i_{AB} supplies two outputs

$$i_{\mathrm{BSf}} = i_{\mathrm{AB}} - I_{\mathrm{BSb}};\qquad i_{\mathrm{AGb}} = i_{\mathrm{AB}} - I_{\mathrm{AGf}} \tag{3}$$

The equation (7) uses odd-even components of the inputs and outputs as follows:

$$I_{\mathrm{s}} = (I_{\mathrm{AGf}} + I_{\mathrm{BSb}})/2;\quad I_{\mathrm{a}} = (I_{\mathrm{AGf}} - I_{\mathrm{BSb}})/2; \tag{4a}$$

$$I_{\mathrm{ABs}} = (I_{\mathrm{BGf}} + I_{\mathrm{ASb}})/2;\ I_{\mathrm{ABa}} = (I_{\mathrm{BGf}} - I_{\mathrm{ASb}})/2 \tag{4b}$$

$$i_{\mathrm{s}} = (i_{\mathrm{ASf}} + i_{\mathrm{BGb}})/2;\qquad i_{\mathrm{a}} = (i_{\mathrm{ASf}} - i_{\mathrm{BGb}})/2$$

$$i_{\mathrm{ABs}} = (i_{\mathrm{BSf}} + i_{\mathrm{AGb}})/2;\quad i_{\mathrm{ABa}} = (i_{\mathrm{BSf}} - i_{\mathrm{AGb}})/2$$

Note that, due to (3), the output i_{ABa} is equal to the odd input I_{a}:

$$i_{\mathrm{ABa}} = (I_{\mathrm{AGf}} - I_{\mathrm{BSb}})/2 = I_{\mathrm{a}} \tag{5}$$

i.e. the first equation in the (7) system.

The inverse transformation

$$i_{\mathrm{ASf}} = i_{\mathrm{s}} + i_{\mathrm{a}};\quad i_{\mathrm{BGb}} = i_{\mathrm{s}} - i_{\mathrm{a}}$$

$$i_{\mathrm{BSf}} = i_{\mathrm{ABs}} + i_{\mathrm{ABa}};\ \ i_{\mathrm{AGb}} = i_{\mathrm{ABs}} - i_{\mathrm{ABa}}$$

$$I_{\mathrm{AGf}} = I_{\mathrm{s}} + I_{\mathrm{a}}:\ \ I_{\mathrm{BSb}} = I_{\mathrm{s}} - I_{\mathrm{a}}$$

$$I_{\mathrm{BGf}} = I_{\mathrm{ABs}} + I_{\mathrm{ABa}};\ I_{\mathrm{ASb}} = I_{\mathrm{ABs}} - I_{\mathrm{ABa}}$$

returns to the terminal variables.

There is a physical interpretation of the introduced currents having parity symmetry. For instance the odd component i_a is a half of the net output current wave charging the winding while the even component i_s is the current output wave traversing the winding.

The equation (7) uses even and odd components of the resistances:

$$\rho_s = (rS + rG)/2,\ \rho_d = (rS - rG)/2$$

Also, there are two constants μ and ν derived from the magnetic coupling ζ. The constant

$$\mu = 2\,\zeta/(1-\zeta^2)$$

is used in

$$\mu / \zeta = 2 + \mu\,\zeta = 2/(1-\zeta^2)$$

or in the equation

$$\mu\,\zeta^2 + 2\,\zeta - \mu = 0$$

for the constant ζ. For $\mu = 2$ this is the equation for the golden ratio $(\sqrt{5} - 1)/2$ while generally

$$\zeta = (\nu-1)/\mu$$

where ν is the other auxiliary constant

$$\nu = \sqrt{1+\mu^2}$$

The constants satisfy identities:

$$\nu = 1+\mu\,\zeta;\ \nu - 1 = \mu\,\zeta;\ \nu + 1 = 2 + \mu\,\zeta = \mu/\zeta \qquad (6)$$

$$1/\zeta - \zeta = (1-\zeta^2)/\zeta = 2/\mu$$

$$(1+\zeta^2)/\zeta = 1/\zeta + \zeta = 1/\zeta - \zeta + 2\zeta = 2/\mu + 2\zeta = 2/\mu(1+\mu\zeta) = 2\,\nu/\mu$$

$$(1+\zeta^2)/(1-\zeta^2) = (1+\zeta^2)/\zeta * \zeta/(1-\zeta^2) = \nu$$

The remaining three equations of the (7) system originate from given input terminal voltages E_S in the node SA in the Figure 2, E_G in the grounding node and the equality of the voltages over the crossover conductor at the node SB in the Figure 2 and analogous node GA at the grounding side of the winding. The original equations include the reflected current waves i_{w0S} and i_{ghS} in the boundary layer at the surge terminal side of the winding and the analogous reflected current waves i_{w0G} and i_{ghG} at the grounding side of the winding. The voltage continuity at nodes BS and AS in the Figure 2 give the two equations for the additional unknowns i_{w0S} and i_{ghS}:

$$-2\,i_{w0S} - \zeta(i_{ASf} - 2i_{ghS} - I_{ASb}) = 0$$

$$-2\,i_{ghS} - \zeta(i_{BSf} - 2\,i_{w0S} - I_{BSb}) = 0$$

with solutions

$$4i_{w0S} = -\,\mu\,i_{ASf} - \mu\zeta\,i_{BSf} + \mu\,I_{ASb} + \mu\zeta\,I_{BSb}$$

$$4i_{ghS} = -\,\mu\zeta\,i_{ASf} - \mu\,i_{BSf} + \mu\zeta\,I_{ASb} + \mu\,I_{BSb}$$

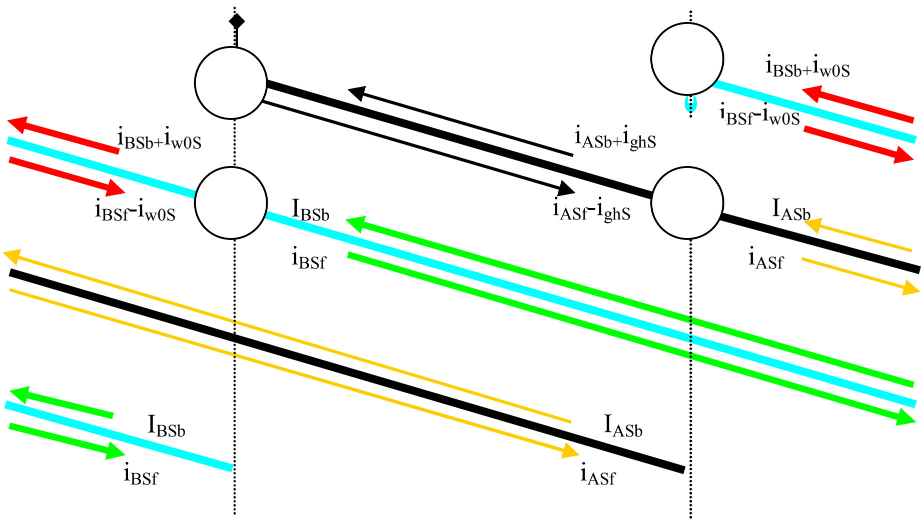

Figure. 2 Input-Output variables at the surge terminal side of the winding

The analogous development at the ground G terminal in the nodes AG and BG gives the equations

$$2\,i_{w0G} - \zeta(2\,i_{ghG} - i_{BGb} + I_{BGf}) = 0;$$

$$2\,i_{ghG} - \zeta(2\,i_{w0G} - i_{AGb} + I_{AGf}) = 0$$

with the solutions

$4i_{w0G}$ = -μ i_{BGb} - μζ i_{AGb} + μ I_{BGf} + μζ I_{AGf}

$4i_{ghG}$ = -μ ζ i_{BGb} - μ i_{AGb} + μ ζ I_{BGf} + μ I_{AGf}

Now the derivation of the remaining three input-output equations in the (7) system is almost straightforward. The last equation, the even counterpart to the odd one, developed in (5) comes from the equality of the voltages over the crossover conductor expressed as

$$(E_{SB} - E_{GA})/2 = 0$$

where the voltages E_{SB} and E_{GA} at the crossover conductor end are given by

$$E_{SB} = (i_{BSf} - 2i_{w0S} - I_{BSb}) + \mu\,(i_{ASf} - I_{ASb})/2 + \mu^*\zeta(i_{BSf} - I_{BSb})/2 = i_{BSf} - 4i_{w0S} - I_{BSb}$$

$$-E_{GA} = (i_{AGb} - 2i_{w0G} - I_{AGf}) + \mu\,(i_{BGb} - I_{BGf})/2 + \mu^*\zeta(i_{AGb} - I_{AGf})/2 = i_{AGb} - 4i_{w0G} - I_{AGf}$$

giving

$$(1 + \mu\zeta)i_{ABs} + \mu\, i_s = (1 + \mu\zeta)\mathrm{Is} + \mu\, I_{ABs}$$

which, according the first identity in (6), is the last equation in (7)

$$\nu\, i_{ABs} + \mu\, i_s = \nu\, I_s + \mu\, I_{ABs}$$

The two companion equations in the middle of the (7) system are obtained by symmetry decomposition of the voltages at the surge node SA and the ground node GB.

$$r_S(i_{ASf} + I_{ASb}) + (i_{ASf} - 2\, i_{ghS} - I_{ASb}) + \mu\,(i_{BSf} - I_{BSb})/2 + \mu\zeta\,(i_{ASf} - I_{ASb})/2 = E_{SA} = E_S$$

$$r_G(i_{BGb} + I_{BGf}) = (2\, i_{ghG} - i_{BGb} + I_{BGf}) + \mu\,(I_{AGf} - i_{AGb})/2 + \mu\zeta\,(I_{BGf} - i_{BGb})/2$$

Substitutions and proper arrangement gives

$$(\nu + r_S)\, i_{ASf} + \mu\, i_{BSf} = (\nu - r_S)\, I_{ASb} + \mu\, I_{BSb} + E_S$$

$$(\nu + r_G)\, i_{BGb} + \mu\, i_{AGb} = (\nu - r_G)\, I_{BGf} + \mu\, I_{AGf}$$

The half difference and the half sum of the previous equations are just the two middle companion equations of the system (7)

$$[L]\begin{bmatrix} i_{ABa} \\ i_a \\ i_s \\ i_{ABs} \end{bmatrix} = [R]\begin{bmatrix} I_{ABa} \\ I_a \\ I_s \\ I_{ABs} \end{bmatrix} + \begin{bmatrix} 0 \\ 1/2 \\ 1/2 \\ 0 \end{bmatrix} E_S \qquad (7)$$

where

$$[L] = \begin{bmatrix} 1 & 0 & 0 & 0 \\ \mu & \nu + \rho_s & \rho_d & 0 \\ 0 & \rho_d & \nu + \rho_s & \mu \\ 0 & 0 & \mu & \nu \end{bmatrix} \qquad (7a)$$

and

$$[R] = \begin{bmatrix} 0 & 1 & 0 & 0 \\ -\nu + \rho_s & -\mu & 0 & -\rho_d \\ \rho_d & 0 & \mu & \nu - \rho_s \\ 0 & 0 & \nu & \mu \end{bmatrix} \qquad (7b)$$

are the left and right matrix coeficient of the equation (7).

IV. STATE SPACE EQUATIONS FOR $\rho_d = 0$

The quasi-stationary input-output (7) lasts until output current waves from one side of the winding become inputs to the other side. This discrete time dynamics can be specified as

$$I_{AGf}(s+1) = i_{ASf}(s),\ I_{BGf}(s+1) = i_{BSf}(s)$$

$$I_{ASb}(s+1) = i_{AGb}(s),\ I_{BSb}(s+1) = i_{BGb}(s)$$

where s means the time step index. One step for the parity symmetric components of (7) consists of the substitution

$$I_{ABa}(s+1) = i_{ABa}(s),\ I_a(s+1) = i_a(s)$$

$$I_s(s+1) = i_s(s),\ I_{ABs}(s+1) = i_{ABs}(s)$$

Let v(s) = E_S and

$$[x(s) = [I(s) = [I_{ABa}, I_a, I_s, I_{ABs}]'(s)$$

Then

$$[x(s+1) = [I(s+1) = [i(s) = [i_{ABa}, i_a, i_s, i_{ABs]}'\ (s)$$

and the system (7) can be converted to the state space equation (1). In particular for ρ_d = 0 the odd and even components are decoupled into two blocks.

The first block describing the odd parity dynamics becomes

$$\begin{bmatrix} x_1(s+1) \\ x_2(s+1) \end{bmatrix} = [A_a]\begin{bmatrix} x_1(s) \\ x_2(s) \end{bmatrix} + [B_a]v(s) \qquad (8)$$

where

$$[A_a] = \frac{1}{\nu + \rho_s}\begin{bmatrix} 0 & \nu + \rho_s \\ -\nu + \rho_s & -2\mu \end{bmatrix}, \quad [B_a] = \frac{1}{\nu + \rho_s}\begin{bmatrix} 0 \\ 1/2 \end{bmatrix}$$

The most noteworthy properties of the (8) dynamics are characteristic (proper) values (eigenvalues, latent roots) of the state transition matrix $[A_a]$ defined as the roots of the characteristic equation

$$\det([A_a] - \lambda[1]) = \lambda^2 + \frac{2\mu}{\nu + \rho_s}\lambda + \frac{\nu - \rho_s}{\nu + \rho_s} = 0$$

i.e.

$$\lambda_1 = \lambda_a, \quad \lambda_2 = \lambda_a^*$$

where

$$\lambda_a = \frac{-\mu + j\sqrt{1-\rho_s{}^2}}{\nu + \rho_s} = \Lambda_a e^{j\varphi_a},$$

$$\Lambda_a = \sqrt{\frac{\nu - \rho_s}{\nu + \rho_s}},$$

$$\cos(\varphi_a) = -\frac{\mu}{\nu^2 - \rho_s{}^2}, \quad \pi/2 \le \varphi_a < \pi$$

and asterisk * denotes complex conjugation. That means the odd parity currents are oscillatory with frequency φ_a and damping ratio $\Lambda_a \approx 1\text{-}\rho_s/\nu$. Dynamics details are obtained with the matrix $[A_a]$ characteristic vectors and their amplitudes in the next section.

The second block, describing the even components dynamics, becomes

$$\begin{bmatrix} x_3(s+1) \\ x_4(s+1) \end{bmatrix} = [A_s]\begin{bmatrix} x_3(s) \\ x_3(s) \end{bmatrix} + [B_s]v(s) \tag{9}$$

where

$$[A_s] = \frac{1}{1+\rho_s\nu}\begin{bmatrix} 0 & 1-\rho_s\nu \\ 1+\rho_s\nu & 2\mu\rho_s \end{bmatrix}, \quad [B_s] = \frac{1}{1+\rho_s\nu}\begin{bmatrix} \nu/2 \\ -\mu/2 \end{bmatrix}$$

The roots of the characteristic equation

$$\det([A_s] - \lambda[1]) = \lambda^2 - \frac{2\mu\rho_s}{1+\nu\rho_s}\lambda - \frac{1-\nu\rho_s}{1+\nu\rho_s} = 0$$

are given by

$$\lambda_3 = \frac{\sqrt{1-\rho_s{}^2} + \mu\rho_s}{1+\nu\rho_s}, \quad \lambda_4 = \frac{-\sqrt{1-\rho_s{}^2} + \mu\rho_s}{1+\nu\rho_s}$$

The λ_3 characteristic value is responsible for the uniform current output wave traversing the winding, dumped as traversing the impedance with the R/L = $1\text{-}\lambda_3$ ratio. The other λ_4 proper values give alternating traversing transient with the larger influence of the resistances to the damping. Details are presented in the next section.

Since the output variables of the state space model (2) do not comprise dynamic characteristics they will not be considered here

V: MODAL ANALYSIS OF THE REDUCED DYNAMICS

This section presents the proper vectors (dynamic modes) for the characteristic values of the transition matrix related with the reduction of the transition matrix to the diagonal form by similarity transformation. This task benefits a lot from the odd component of resistances ρ_d being set to zero so that the transition matrix is advantageously partitioned into uncoupled 2×2 blocks.

The similarity transformation of the first block $[A_a]$ to the diagonal form is related to the search of proper vectors [ψ which satisfy

$$[A_a]\,[\psi = \lambda\,[\psi$$

Proper vectors exist when the parameter λ is a proper value i.e. the root of the characteristic equation. The two proper vectors for the roots λ_a and λ_a^* are presented as the columns of the matrix

$$[\Psi_a] = \begin{bmatrix} 1 & 1/\lambda_a^* \\ \lambda_a & 1 \end{bmatrix} \tag{10}$$

so that

$$[A_a][\Psi_a] = [\Psi_a]\begin{bmatrix} \lambda_a & 0 \\ 0 & \lambda_a^* \end{bmatrix}$$

or

$$[\Psi_a]^{-1}[A_a][\Psi_a] = \begin{bmatrix} \lambda_a & 0 \\ 0 & \lambda_a^* \end{bmatrix} \tag{11}$$

The inverse of the transformation matrix $[\Psi_a]$ is

$$[\Psi_a]^{-1} = \frac{\lambda_a^*}{\lambda_a^* - \lambda_a}\begin{bmatrix} 1 & -1/\lambda_a^* \\ -\lambda_a & 1 \end{bmatrix}$$

The similarity transformation that reduces $[A_a]$ to diagonal form is the consequence of the representation of the state vector in the proper vectors (columns of $[\Psi_a]$) basis:

$$\begin{bmatrix} x_1 \\ x_2 \end{bmatrix} = [\Psi_a]\begin{bmatrix} \xi_1 \\ \xi_2 \end{bmatrix} \tag{12}$$

The uncoupled dynamics of the modal amplitudes comes from (9) substituting (12), left multiplying with $[\Psi_a]^{-1}$ and applying (11):

$$\begin{bmatrix} \xi_1(t+1) \\ \xi_2(t+1) \end{bmatrix} = \begin{bmatrix} \lambda_a & 0 \\ 0 & \lambda_a^* \end{bmatrix}\begin{bmatrix} \xi_1(t) \\ \xi_2(t) \end{bmatrix} + \frac{jE_S(t)}{4\sqrt{1-\rho_s^2}}\begin{bmatrix} -1 \\ \lambda_a^* \end{bmatrix}$$

The second term gives the excitation of the modal amplitudes by the surge voltage E_S. The modal amplitudes are complex since modal vectors in (10) are complex. The modal synthesis (12) gives back the real state space variables. Actually the two modes are inseparable in (9) but when iterated it is advantageous to use the modal analysis for the explicit potential of the transition matrix:

$$[A_a]^n = [\Psi_a]\begin{bmatrix} \lambda_a^n & 0 \\ 0 & \lambda_a^{*n} \end{bmatrix}[\Psi_a]^{-1}$$

The similarity transformation of the second block $[A_s]$ to the diagonal form is analogous to the transformation of the first block. The columns of the transformation matrix $[\Psi_b]$ are proper vectors of the transition matrix $[A_s]$ or the null vectors of

$$[A_s] - \lambda_3[1] = \begin{bmatrix} -\lambda_3 & -\lambda_3\lambda_4 \\ 1 & \lambda_4 \end{bmatrix}$$

and

$$[A_s]-\lambda_4[1]=\begin{bmatrix}-\lambda_4 & -\lambda_3\lambda_4\\ 1 & \lambda_3\end{bmatrix}$$

For instance

$$[\Psi_s]=\begin{bmatrix}-\lambda_4 & -\lambda_3\\ 1 & 1\end{bmatrix}$$

gives

$$[\Psi_s]^{-1}=\frac{1}{\lambda_3-\lambda_4}\begin{bmatrix}1 & \lambda_3\\ -1 & -\lambda_4\end{bmatrix}$$

and

$$[\Psi_s]^{-1}[A_s][\Psi_s]=\begin{bmatrix}\lambda_3 & 0\\ 0 & \lambda_4\end{bmatrix}$$

With

$$\begin{bmatrix}x_3\\ x_4\end{bmatrix}=[\Psi_s]\begin{bmatrix}\xi_3\\ \xi_4\end{bmatrix}$$

the (8) transforms to the modal state space equations

$$\begin{bmatrix}\xi_3(t+1)\\ \xi_4(t+1)\end{bmatrix}=\begin{bmatrix}\lambda_3 & 0\\ 0 & \lambda_4\end{bmatrix}\begin{bmatrix}\xi_3(t)\\ \xi_4(t)\end{bmatrix}+\begin{bmatrix}\nu-\lambda_3\mu\\ -\nu+\lambda_4\mu\end{bmatrix}\frac{E_S(t)}{4\sqrt{1-\rho_s^2}}$$

Here it comes out that

$$\begin{bmatrix}\nu-\lambda_3\mu\\ -\nu+\lambda_4\mu\end{bmatrix}=\frac{\nu+\rho_s}{1+\rho_s\nu}\begin{bmatrix}1\\ -1\end{bmatrix}-\frac{\mu\sqrt{1-\rho_s^2}}{1+\rho_s\nu}\begin{bmatrix}1\\ 1\end{bmatrix}.$$

VI. CONCLUSION

. Although the fast transients significantly modify quasi-stationary states in the later steps, the reduced model still gives the valid dynamical component which could be responsible for experimentally and numerically established surge transient oscillations [2] in interleaved windings. The transparency of the results comes out from the several key suppositions. The first one is the interleaved connection of the winding shown in the Figure. 1. The initial connection a) results in a favorable multi-conductor transmission line model of the interleaved helical winding. The modified one b) is still more advantageous without the loss of quality. The TEM supposition and exponential approximation of the mutual inductances are essential for getting the small (four) rank quasi-stationary states system. The additional advantage comes from odd-even symmetry decomposition capable to incorporate the effects of the resistances. The transition matrices of symmetric components are not only of the low (second) order but also have properties that makes easy to find the proper values and proper vectors (modes).

The obtained results should be compared with analogous results for the much simpler case of non-interleaved windings.

REFERENCES

[1] B. Heller and A. Veverka, *Surge phenomena in electrical machines*, London: Iliffe Books, 1968

[2] K. Cornick, B. Filliat, C.Kieny and W. Muller: *Distribution of very fast overvoltages in transformer windings*, Report 12-204 CIGRE Paris, 1992

[3] P. Bodlovic, K. Hot and T.Kelemen *: Basic Travelling Waves in Interleaved Transformer Windings*, ISEF 2003, - 11th International Symposium on Electromagnetic Fields in Electrical Engineering, Maribor, Slovenia, September 18-20, 2003

[4] H. Kwakernaak, R. *Sivan Linear Optimal Control Systems*, Wiley-Interscience I972, Translation to russian Mir, Moskva 1977

[5] J.H. Wilkinson: *The Algebraic Eigenvalue Problem*, Clarendon Press, Oxford 1965.